Earthq Eng & Eng Vib (2017) 16: 247-261 **DOI**:10.1007/s11803-017-0380-2

Shear wave velocity-based evaluation and design of stone column improved ground for liquefaction mitigation

Zhou Yanguo[†], Sun Zhengbo[‡], Chen Jie[§], Chen Yunmin[*], Chen Renpeng[*]

MOE Key Laboratory of Soft Soils and Geoenvironmental Engineering, Institute of Geotechnical Engineering, Zhejiang University, Hangzhou 310058, China

Abstract: The evaluation and design of stone column improvement ground for liquefaction mitigation is a challenging issue for the state of practice. In this paper, a shear wave velocity-based approach is proposed based on the well-defined correlations of liquefaction resistance (CRR)-shear wave velocity (V_s)-void ratio (e) of sandy soils, and the values of parameters in this approach are recommended for preliminary design purpose when site specific values are not available. The detailed procedures of pre- and post-improvement liquefaction evaluations and stone column design are given. According to this approach, the required level of ground improvement will be met once the target V_s of soil is raised high enough (i.e., no less than the critical velocity) to resist the given earthquake loading according to the CRR-V_s relationship, and then this requirement is transferred to the control of target void ratio (i.e., the critical e) according to the V_s-e relationship. As this approach relies on the densification of the surrounding soil instead of the whole improved ground and is conservative by nature, specific considerations of the densification mechanism and effect are given, and the effects of drainage and reinforcement of stone columns are also discussed. A case study of a thermal power plant in Indonesia is introduced, where the effectiveness of stone column improved ground was evaluated by the proposed V_s-based method and compared with the SPT-based evaluation. This improved ground performed well and experienced no liquefaction during subsequent strong earthquakes.

Keywords: Liquefaction mitigation; Stone column; Shear wave velocity; Void ratio; Densification; Ageing effect

1 Introduction

Soil liquefaction during earthquakes will induce a loss of bearing capacity and significant deformation of ground, which causes damage and failure of infrastructures (Wang *et al.*, 2002, 2010; Yuan and Cao, 2001; Pan *et al.*, 2011; Tang *et al.*, 2014; Zhou *et al.*, 2014; Chen *et al.*, 2015). Liquefaction remediation methods such as densification (Seed and Booker, 1977), drainage (Howell *et al.*, 2012; JGS, 1998) and solidification (Conlee *et al.*, 2012) are widely used in engineering practices. Stone column was proved cost effective for liquefaction mitigation in sandy deposits (Mitchell *et al.*, 1995; Baez, 1995; Adalier and Elgamal, 2004). The stone column mitigates the liquefaction potential by increasing the density of surrounding soil, improving the drainage capacity and providing reinforcement (i.e., to reduce shear stress levels in the surrounding soil) (see Fig. 1).

Liquefaction evaluation before and after improvement and seismic design of stone column are the main concerns of liquefaction mitigation. Field test such as the Standard Penetration Test (SPT) and the Cone Penetration Test (CPT), are widely used because of the extensive databases and past engineering experiences (NEHRP, 2003; Samui 2007). In common practices of stone column design, the critical blow count (or cone penetration resistance) is taken as the control parameter to determine the construction choices (i.e., spacing and diameter of stone column). However, such method depends mainly on empirical models and field penetration index to determine the construction choices at a given site (Baez and Martin, 1992; Shenthan *et al.*, 2004), where the normalized SPT blow count $(N_1)_{60}$ or the

Correspondence to: Chen Yunmin , MOE Key Laboratory of Soft Soils and Geoenvironmental Engineering, Institute of Geotechnical Engineering, Zhejiang University, Hangzhou 310058, China
Tel: +86-571-88208776 (o); Fax: +86-571 88208793 (o)
E-mail: chenyunmin@zju.edu.cn

[†]Associate professor; [‡]PhD Candidate; [§]Graduate student; [*]Professor

Supported by: National Natural Science Foundation of China under Grant No. 51578501 and No. 51127005; the Foundation for the Author of National Excellent Doctoral Dissertation of P R China under Grant No. 201160; the Zhejiang Provincial Natural Science Foundation of China under Grant No. LR15E080001; the National Basic Research Program of China (973 Project) under Grant No. 2014CB047005; the Fundamental Research Funds for the Central Universities under Grant No. 2014FZA4016 and Zhejiang University K. P. Chao's High Technology Development Foundation (2014)

Received June 4, 2016; **Accepted** February 17, 2017

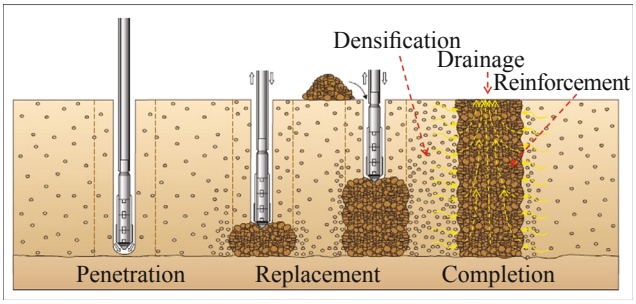

Fig. 1 Stone column construction by vibro-replacement (modified from Hayward Baker, 2004)

normalized CPT cone penetration resistance q_{c1N} do not relate to the liquefaction resistance directly. Liquefaction resistance of granular soils is commonly characterized by the cyclic resistance ratio (CRR) in the simplified shear stress procedure of liquefaction potential assessment, and this parameter can be determined using cyclic tests on the undisturbed or reconstituted laboratory specimens (Youd *et al*., 2001).

Recently, the use of shear wave velocity (V_s) as a field index of CRR becomes prevailing, in view of the fact that V_s and CRR are similarly influenced by void ratio, effective confining stresses, stress histories, and geologic age, etc. (Andrus and Stokoe, 2000; Juang *et al*., 2001; Cai *et al*., 2012). As V_s relate to shear modulus directly, soil with larger modulus tends to deform less under the same cyclic shear stress, and therefore the shear strain and liquefaction will develop slower (Wang, 2001). Thus V_s provides a physically meaningful index to evaluate CRR and the associated consequences (Özener, 2012), and has been adopted in recent seismic design codes (GB50487-2008, Eurocode 8, NUREG/CR-5741, etc.). Besides, V_s is also a key parameter for seismic response analysis of improved ground (Stuedlein *et al*., 2015). Therefore shear wave velocity is a promising alternative index for liquefaction evaluation and seismic design of stone column improved ground.

This paper provides one innovative design procedure to determine the construction choices in liquefiable soils treated by stone columns based on the correlations among liquefaction resistance (CRR), shear wave velocity (V_s) and void ratio (e) of sandy soils. According to this approach, the post-improvement ground is supposed to meet requirement once the target shear wave velocity is reached, and such requirement could be readily transferred to the required void ratio, and guiding the construction choices during stone column design. A case study of thermal power plant is introduced, where down-hole test and SPT tests were performed to assess the liquefaction resistance before improvement. Stone columns were designed to mitigate liquefaction according to the proposed approach. SPT tests were conducted in the treated area and the liquefaction potential of the improved ground were evaluated. The effectiveness of stone column improved ground in this project was proved by recent strong earthquakes.

2 Shear wave velocity-based liquefaction evaluation

The simplified procedure for liquefaction evaluation was developed from empirical evaluations of field observations, field testing and laboratory test data (Seed and Idriss, 1971). The factor of safety (FS) against liquefaction is the ratio between liquefaction resistance ratio (CRR) of the soil and cyclic stress ratio (CSR) induced by earthquake loading:

$$\mathrm{FS} = \mathrm{CRR}/\mathrm{CSR} \tag{1}$$

The site will experience liquefaction when FS < 1, and liquefaction mitigation like stone column is required for ground improvement.

According to Seed and Idriss (1971), CSR at a given depth can be estimated as:

$$\mathrm{CSR} = \frac{\tau_{\mathrm{av}}}{\sigma'_{\mathrm{v0}}} = 0.65\left(\frac{a_{\max}}{g}\right)\left(\frac{\sigma_{\mathrm{v0}}}{\sigma'_{\mathrm{v0}}}\right) r_{\mathrm{d}} \tag{2}$$

where $a_{\max}$ = peak horizontal acceleration at the ground surface; g = acceleration of gravity; σ_{v0} and σ'_{v0} = total and effective vertical overburden stresses, respectively; and r_{d} = shear stress reduction coefficient.

As far as the determination of CRR is considered, several V_s-based liquefaction evaluation methods have been recommended in seismic design codes. For example, Eurocode 8 (1998) proposes the empirical liquefaction charts with shear wave velocity versus CRR to assess liquefaction according to Robertson *et al*. (1992). NUREG/CR-5741 (2000) suggests a CRR-V_{s1} correlation to assess the liquefaction potential that is also recommended by NCEER (Andrus and Stoke, 2000) as follows:

$$\mathrm{CRR} = a\left(\frac{V_{s1}}{100}\right)^2 + b\left(\frac{1}{V^*_{s1} - V_{s1}} - \frac{1}{V^*_{s1}}\right) \tag{3}$$

where V^*_{s1} = limiting upper value of V_{s1} for liquefaction occurrence, is 215 m/s for clean sand; and a and b are curve fitting parameters from field case histories. In Chinese codes, GB50487-2008 recommends a equation for evaluation of liquefaction susceptibility based on cyclic threshold strain, and GB50021-2001 recommends a critical shear wave velocity V_{scr} at a specific depth d_s for no liquefaction occurrence as follows:

$$V_{\mathrm{scr}} = V_{s0}\left(d_s - 0.0133 d_s^2\right)^{0.5}\left[1.0 - 0.185\left(\frac{d_w}{d_s}\right)\right]\left(\frac{3}{\rho_c}\right)^{0.5} \tag{4}$$

where V_{s0} = the empirical parameter, d_w = depth of ground water level.

It should be noted that most of the existing V_s-based methods are developed from the concept of cyclic threshold strain instead of initial liquefaction (Dobry *et al*. 1982; Andrus and Stokoe, 2000) and also suffers the problem of insufficient liquefaction field case histories compared with SPT and CPT, especially in zones of high CSR and high V_s (Kayen *et al*., 2013). This problem makes it difficult to apply cost-effective ground improvement in highly seismic active areas. To address this problem, the present authors proposed a semi-theoretical CRR-V_s correlation for sandy soils (Zhou and Chen, 2007):

$$\mathrm{CRR} = r_c \frac{1}{P_a}\left[\frac{k_N \rho}{F(e_{\min})}\right]^{1/n} (V_{s1})^{2/n} \tag{5}$$

where r_c = a constant of multidirectional shaking (0.9-1.0); P_a = reference overburden stress (= 100 kPa); k_N = fitting value for a given failure cycle number N from cyclic triaxial test, and the lower bound values of k_N are recommended in Table 1 for preliminary use; n = power exponent in Hardin equation; $e_{\min}$ = minimum void ratio and $F(e)$ is void ratio function, $F(e) = 1/(0.3+0.7e^2)$; ρ = total mass density of the soil.

This CRR-V_{s1} correlation predicts that liquefaction resistance will vary proportionally to the $2/n$ power of V_{s1}, which was verified by comprehensive laboratory tests, centrifuge tests and field case histories (Zhou *et al.*, 2009, 2010). Figure 2 compares the CRR-V_{s1} curve with several other curves recommended by Eurocode 8, NUREG/CR-5741, Japanese researchers (Tokimatsu and Uchida, 1990) and Chinese codes (GB50487-2008 and GB50021-2001). It can be seen that the proposed curve is a slightly downward departure from the previous international V_s studies based on field case histories, in that it characterized the loading conditions at high CSR levels in a controlled laboratory setting. Meanwhile, the curves provided by Chinese codes for the case of a saturated sand deposit at depth of 10 m are significantly conservative as they essentially developed from the concept of cyclic threshold strain (Shi *et al.*, 1993), which criterion is different from the initial liquefaction that adopted by the proposed curve.

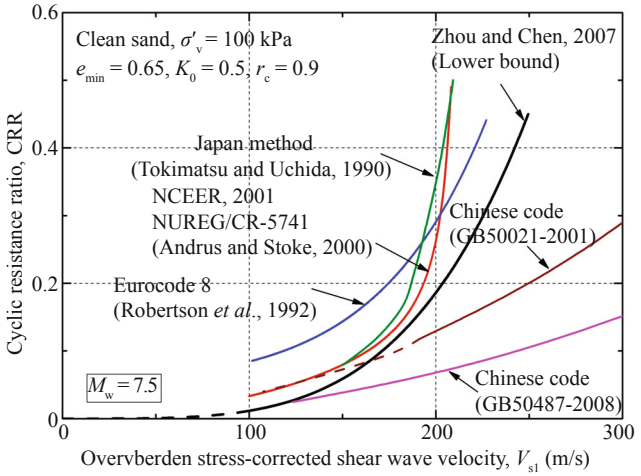

Fig. 2 Comparison between different CRR-V_{s1} curves in design codes

When a site is evaluated liquefaction under a given earthquake, the critical shear wave velocity (V_{scr}) for liquefaction triggering is estimated by equaling CRR to CSR in Eq. (2), and given by:

$$V_{scr} = \left[\frac{0.65}{r_c} P_a \left(\frac{a_{max}}{g}\right)\left(\frac{\sigma_{v0}}{\sigma'_{v0}}\right)\left(\frac{F(e_{\min})}{k_N \rho}\right)^{1/n} r_d\right]^{n/2} \tag{6}$$

On the average, $e_{\min}$ is 0.65 for sand with fines content (FC) less than 20%, 0.75 for silty sand and 0.95 for sandy silt (Tokimatsu and Uchida, 1990). Besides, Aboshi *et al*. (1991) also proposed a similar relationship between $e_{\min}$ and FC as $e_{\min} = 0.6+0.008\mathrm{FC}$. Such relations may be used as the first approximation when soil-type specific $e_{\min}$ is unavailable.

3 Stone column design for liquefaction mitigation

When the stone column design is considered, V_s is well related to void ratio (e) and mean effective stress by Hardin equation (i.e., $G_{max} = AF(e)(\sigma'_m)^n$, Hardin and Richart, 1963), so the requirement of critical V_s value to resist liquefaction could be transferred to the requirement of critical e value at a given depth, then the corresponding construction choices could be proceeded. This section aims at proposing the V_s-based stone column design

Table 1 Lower bound value of k_N (10^{-4} kPa$^{-0.5}$) for different sandy soils

Earthquake magnitude, M_w	Equivalent failure cycles, N	Clean sand FC ≤ 5%	Silty sand 5% < FC < 35%	Silty sand FC ≥ 35%
8.50	26	0.932	0.912	0.938
7.50	15	0.997	0.959	0.982
6.75	10	1.073	1.024	1.042
6	5	1.173	1.113	1.132
5.25	3	1.300	1.216	1.225

Note: The V_s-e correlation may not applicable for very shallow depth (e.g., d < 1 m).

procedure, and provides comprehensive considerations with regard to the improvement mechanisms and design safety.

3.1 Determination of critical void ratio by critical velocity

For sandy soil, a formula of G_{max} at shear strain of 10^{-4} or less similar to Hardin equation was proposed by Wichtmann and Triantafyllidis (2009):

$$G_{max} = AF(e)(\sigma'_m)^n (P_A)^{1-n} \tag{7}$$

where A = a constant of material property; $\sigma'_m = \sigma'_{v0}(1+2K_0)/3$, the mean effective stresses; K_0 = the coefficient of earth pressure at rest, in general is assumed 0.5. According to theory of elasticity, small-strain modulus relates to shear wave velocity by:

$$G_{max} = \rho V_s^2 \tag{8}$$

By combining Eqs. (7) and (8) with $F(e) = 1/(0.3+0.7e^2)$, e can be expressed in terms of V_s as follows:

$$e = \sqrt{\frac{1}{0.7}\cdot\left[\frac{A(\sigma'_m)^n (P_A)^{1-n}}{\rho V_s^2} - 0.3\right]} \tag{9}$$

Equation (9) implies that e will almost decrease with the increase of soil V_s linearly. Some typical soil-type specific V_s-e correlations proposed by previous studies are shown in Fig. 3 (Huang *et al.*, 2004; Wichtmann and Triantafyllidis, 2009; Paydar and Ahmadi, 2014). Table 2 recommends the average values of A and n based on literature review. The value of A decreases significantly as FC increases, while n almost remains the same for sandy soil (i.e., $n \approx 0.5$, Lo Presti, 1987). Note that the regressed values should be less reliable

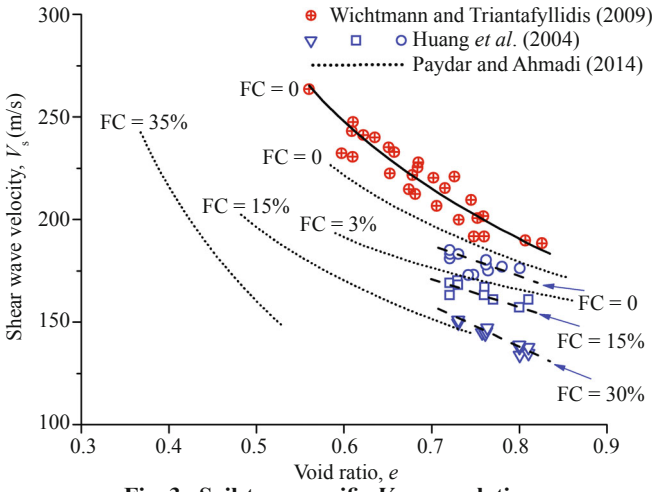

Fig. 3 Soil-type specific V_s-e correlations

Table 2 Value of A (10^2) and n for different sandy soils

Parameter	Clean sand (FC ≤ 5%)	Silty sand (5%<FC<35%)	Silty sand (FC≥35%)
A	5.56	4.04	2.00
n	0.49	0.51	0.58

for sandy soils with large fines content due to the insufficient datasets (Salgado *et al.*, 2000; Dabiri *et al.*, 2011). As the values in Table 2 are only for preliminary design purpose, it is always recommended to obtain the soil type specific parameters by laboratory tests with V_s measurement for important projects. Then the critical void ratio e_{cr} corresponding to the critical shear wave velocity V_{scr} can be estimated as follows:

$$e_{cr} = \sqrt{\frac{1}{0.7}\cdot\left[\frac{A(\sigma'_m)^n}{\rho V_{scr}^2} - 0.3\right]} \tag{10}$$

Generally, the change of stress level at the same depth is assumed small before and after stone column installation, thus the estimated e_{cr} by Eq. (10) would be reliable.

3.2 Stone column design

There are two general patterns in stone column installations: one is square and the other is triangular, where the spacing and diameter are L and d respectively (see Fig. 4).

The densification effect can be characterized by the change from initial void ratio (e_0) to the average void ratio (e_1) after improvement. Assuming that the vertical settlement after improvement is very small compared to the depth of improvement, one may readily obtain the average void ratio e_1 after improvement. Note that the least requirement of qualified ground improvement is e_1 equals the critical void ratio e_{cr}, then the minimum diameter-to-spacing ratio d/L can be obtained readily by:

$$\frac{d}{L} = \sqrt{\frac{4}{\pi}\frac{e_0 - e_{cr}}{1+e_{cr}}} \tag{11}$$

for square pattern and

$$\frac{d}{L} = \sqrt{\frac{6}{\sqrt{3}\pi}\frac{e_0 - e_{cr}}{1+e_{cr}}} \tag{12}$$

for triangular pattern, respectively.

Figure 5 shows a flowchart for the design of stone column improved ground. For the site of interest: 1) cross-hole or down-hole test is performed to obtain V_s profile; 2) CSR and CRR are determined by Eq. (2) and

Fig. 4 Installation pattern of stone columns: (a) square; (b) triangular

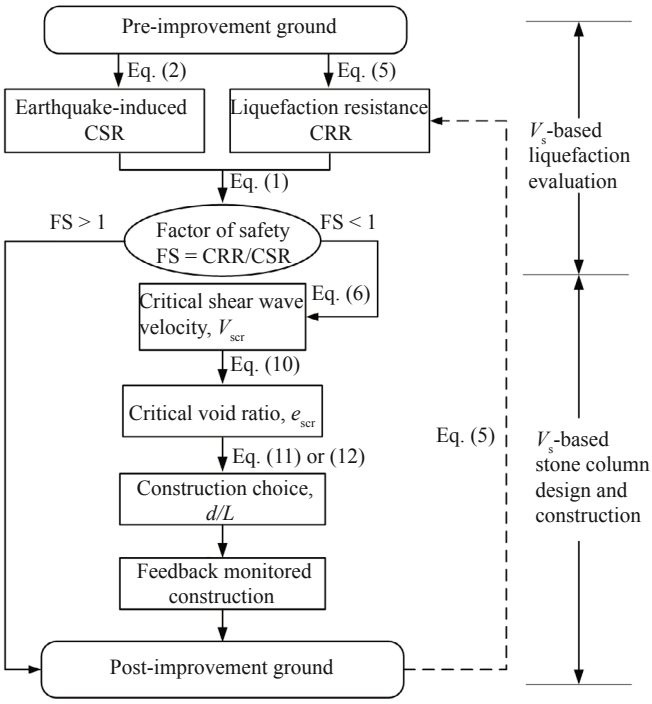

Fig. 5 Flowchart for V_s-based liquefaction evaluation and design of stone column

Eq. (5) respectively, with the aid of Table 1; 3) if the factor of safety FS (Eq. (1)) is less than 1, the site is evaluated liquefaction and stone column improvement is required; 4) V_{scr} and e_{cr} are estimated by Eq. (6) and Eq. (10) respectively, with the aid of Table 2 or element test; 5) The diameter-to-spacing ratio d/L of stone column is obtained by Eq. (11) or Eq. (12); 6) After improvement, V_s test is suggested to check whether the required CRR is obtained or not.

3.3 Other design considerations

The existing design of stone column mainly relies on the mechanism of ground densification induced by stone column (Liu *et al.* 2000), and the improvement effect is generally evaluated in terms of the increase of density. Although the effects of drainage and ground reinforcement (Zhang and Zhang, 2008; Jin *et al.*, 2008; Tang *et al.*, 2015) are not included in the present design, they are treated as additional safety margin. And the actual factor of safety of improved ground could be expected higher than the designed. There are several issues worth further discussions with regard to the design safety:

First, for the main mechanism of densification, there are two issues should be kept in mind: One is the possible change of stress state (i.e., the variation of K_0) after densification, which might also contribute to the increase of liquefaction resistance. For example, when the sand compaction pile (SCP) method is implemented to improve loose sandy deposits, an additional advantage can be expected to occur due to concurrent increase in lateral stress (Harada *et al.*, 2010). The other is the choice of appropriate time for post-improvement field testing to evaluate the densification. Although being densified, sandy deposits may undergo a concurrent loss of stiffness and strength induced by construction disturbance, and exhibit substantial recovery with time up to several months (Mitchell and Solymar, 1984; Lukas 1997; Huang *et al.*, 1992), so the time-dependent behavior (or ageing effect) of the surrounding soil should be recognized properly to choose the right time of post-improvement testing. Besides, in some cases, the installation of precast piles in the improved ground will provide possible additional improvement effects, such as the pile-pinning effect and the restraining the deformation of the liquefiable soils in-between (Elgamal *et al.*, 2009). Engineering experiences show that sandy deposits with fines content less than 15% and clay content less than 2% will be densified due to the installation of piles (Iyengar, 1981). According to Chinese Code for Seismic Design of Buildings (GB50011-2010), these two effects could be considered when the pile spacing is about 2.5–4.0 times of pile diameter and the total number of piles is not less than 5 × 5.

Second, the stone column offers drainage and helps the dissipation of excess pore pressure when earthquake occurs. Large shaking table tests results show that the drainage system is quiet efficient if excess pore pressure ratio (r_u) is lower than a threshold (e.g., r_u = 0.5), and the efficiency decreases as r_u increases at high input

acceleration levels (Iai *et al*., 1988). However, it is difficult to estimate the permeability of the stone column at site. Some study showed that during installation, the stone is mixed with in situ soil, and the final drainage is comprises of about 20% in situ soil (Boulanger *et al*., 1998). Besides, the possibility of further clogging inside the stone column caused by migration of fine particles (Deb and Shiyamalaa, 2015) threatens the long term performance of drainage especially after multiple earthquakes.

Third, the reinforcement effect is often expected based on the assumption that the stone column and surrounding soil have shear strain-compatible deformation. Under this assumption, the columns is believed to undertake higher shear stress, thereby causing a reduction in stress levels in the surrounding soil (Durgunoglu, 2006). However, recent numerical analysis and centrifuge model tests show that the shear reinforcement mechanism of columns was not effective in reducing cyclic stress ratios in the treated soil unless the pile tips could be fixed at the base layer. Therefore the shear strain compatibility assumption can be significantly unconservative and the shear reinforcement of stiffer discrete columns is less effective than commonly used in current design practice (Rayamajhi *et al*., 2012, 2015).

4 Case study

In this section, the liquefaction mitigation and foundation design of a thermal power plant in Indonesia is given as an example of site specific design of V_s-based stone column as proposed above. All parameters used in the following calculations are site specific and obtained by fielding investigation or laboratory testing, conducted by the authors or provided by the project owner.

4.1 Seismicity and site conditions

The thermal power plant is located in Cilacap, southwestern of Central Java, Indonesia (Fig. 6). Probabilistic seismic hazard analysis shows that peak base-rock acceleration for the site is 0.29 g for 475 years return period earthquake, and the peak ground acceleration is 0.30 g according to site response analysis.

The typical soil profile and field indexes are shown in Table 3. Figure 7 shows the SPT-*N* values and V_s profile from down-hole test. The site is prone to liquefaction

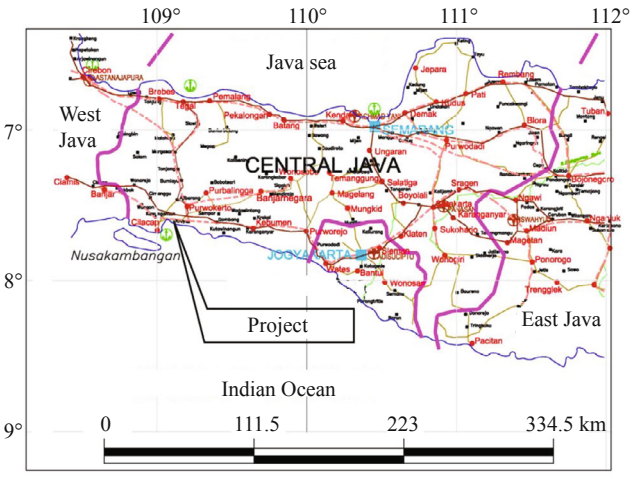

Fig. 6 Location of project site

at the depth of 0.1–16.8 m. It should be noted that the sandy soils are originated from volcanic soils and has considerable bonding/ageing effect, and laboratory result shows the *n* value (0.6–0.65) is slightly larger than normal types of sands, which is consistent with the findings of Yamashita *et al*. (2003).

4.2 Pre-improvement liquefaction evaluation

According to report of seismic hazard analysis provided by the owner of this project, the ground motion information for different return period earthquakes is listed in Table 4. Figure 8 shows the pre-improvement liquefaction evaluations for different earthquake return periods by the proposed method. The V_s- and SPT-based evaluations recommended by NCEER are also

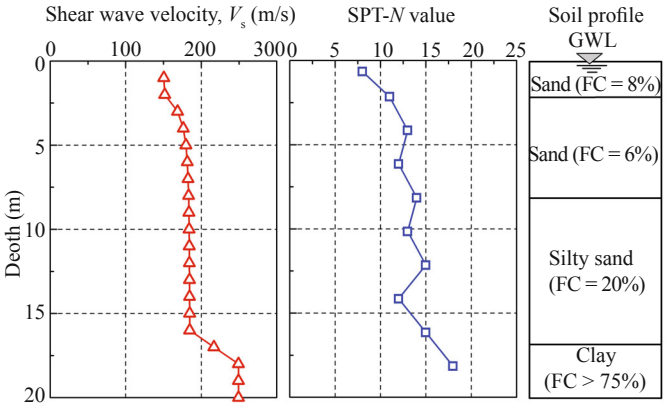

Fig. 7 Typical V_s profile and SPT-*N* values in the field before improvement

Table 3 Soil profile and main indexes

Layer	Depth (m)	USCS chart	Soil type	FC (%)	D_{60} (mm)	D_{10} (mm)	U_C	Description
1	0.0–2.0	SP	Sand	8	0.42	0.19	2.2	Loose
2	2.0–8.0	SP	Sand	6	0.43	0.17	2.5	Medium dense
3	8.0–16.8	SM	Silty sand	20	0.19	0.08	2.4	Medium dense
4	16.8–21.0	CH	Clay	>75	-	-	-	Stiff

Table 4 Earthquake information for different return periods

Earthquake return period (years)	Earthquake magnitude M_w	Peak ground acceleration a_{max}	Magnitude scaling factor (MSF)
50	6.5	0.095 g	1.44
100	6.7	0.140 g	1.33
200	6.8	0.200 g	1.28
475	7.1	0.300 g	1.15

plotted in the figures for comparison. Take Fig. 8(a) as an example, from the left to the right, there are profiles of SPT blow counts (the measured and the overburden corrected), shear wave velocities (the measured and the overburden corrected), CSR induced by 50 years return period earthquake and CRR values estimated by different methods, the corresponding factor of safety by different methods and the soil strata, respectively. The prediction shows that, the site will experience no liquefaction under 50 years return period earthquake,

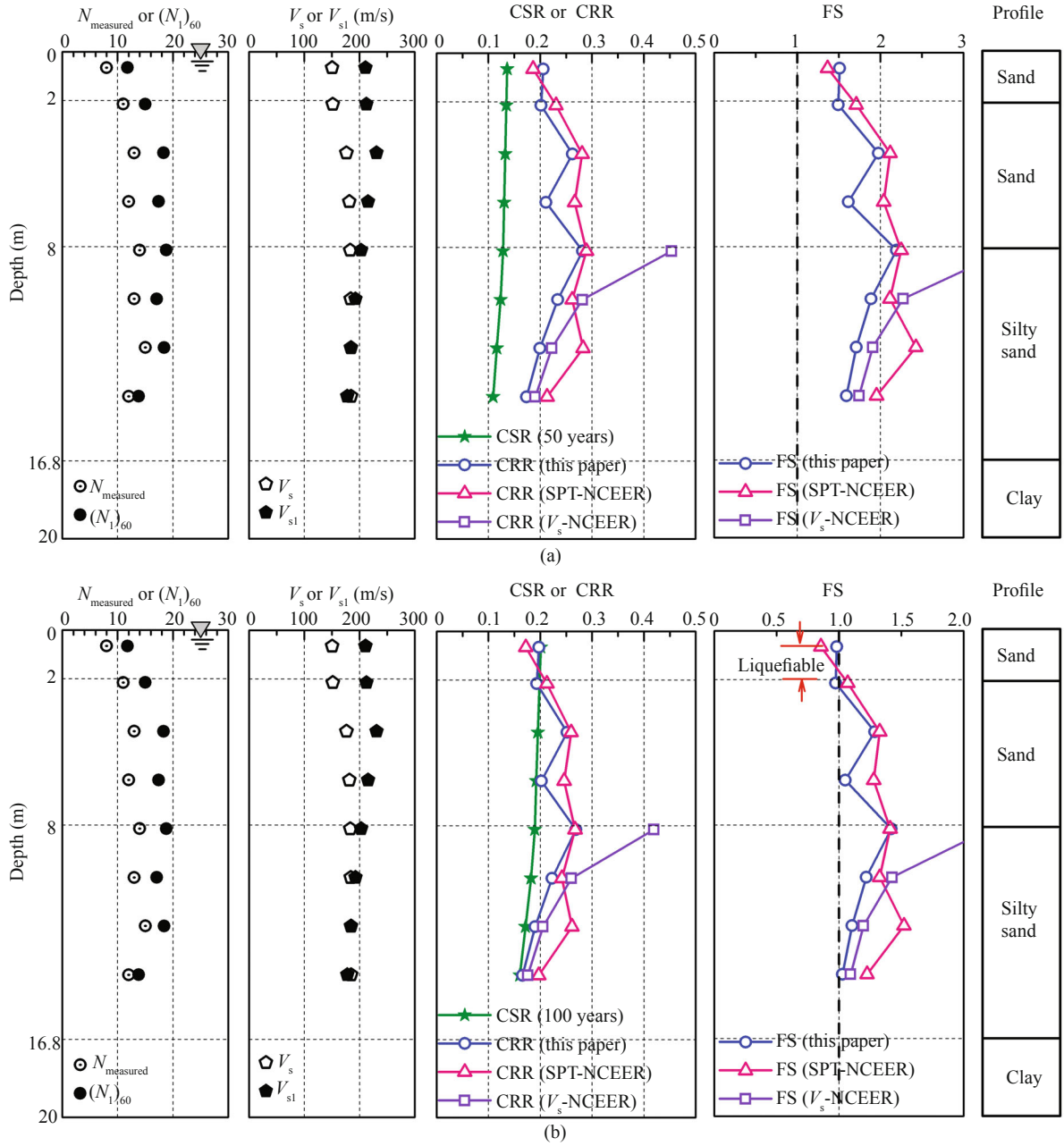

Fig. 8 Pre-improvement liquefaction evaluation for different earthquake return periods: (a) 50 years; (b) 100 years; (c) 200 years; (d) 475 years

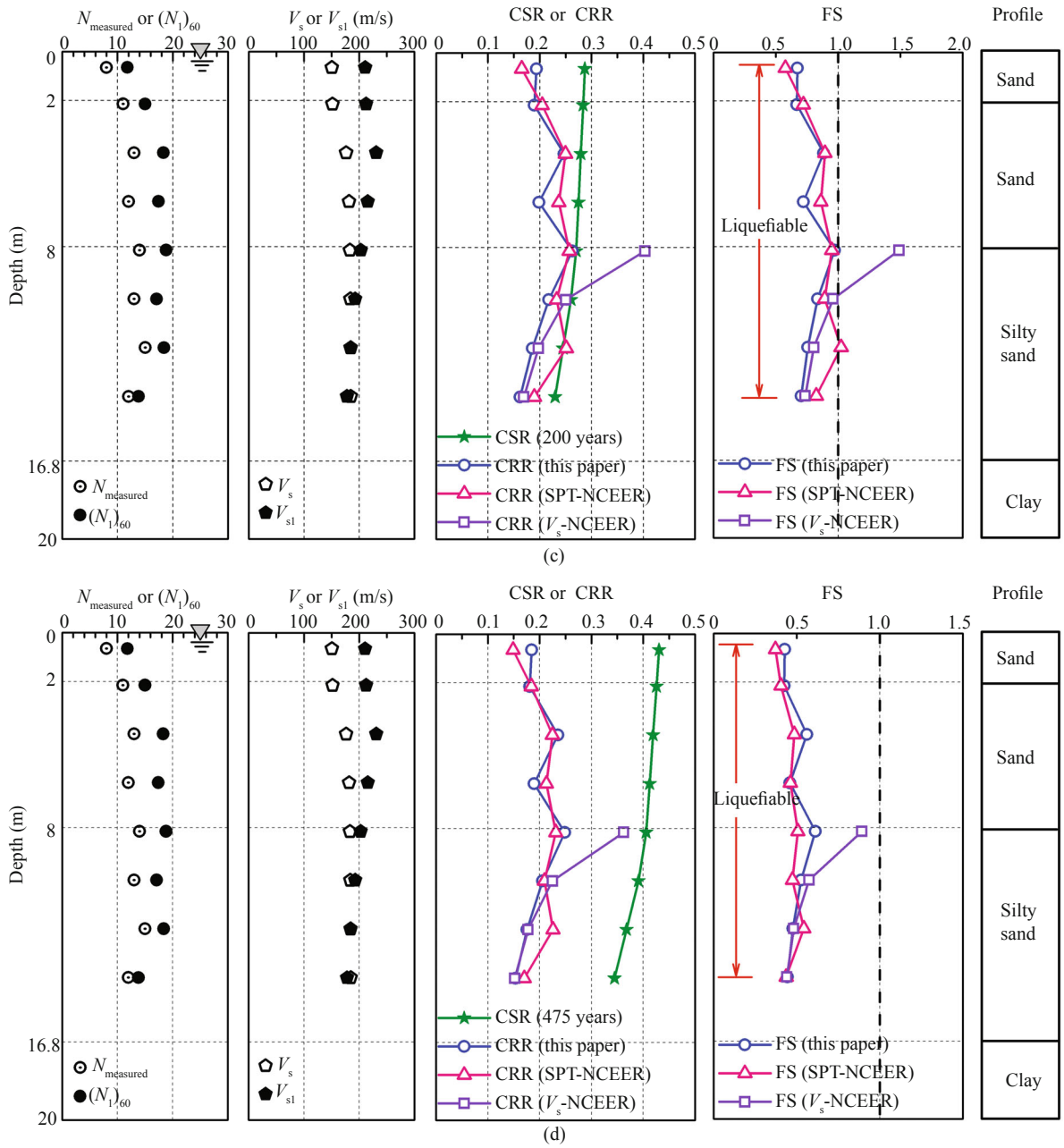

Fig. 8 Continued

and layer 1 (0.5 to 20 m depth) will liquefy for 100 years return period earthquake, and then the whole deposits will liquefy for 200 years and 475 years return period earthquakes. Generally, the predictions are consistent between the proposed CRR-V_{s1} curve and the NCEER SPT-based method. However, the NCEER V_s-based method significantly overestimated the liquefaction resistance for soil layers with large velocities. Note that the normalized velocities at depth of 4.15 m and 6.15 m are larger than the so-called limiting upper value and evaluated as non-liquefaction by NCEER V_s-based method.

4.3 Design and construction of stone column and pile foundation

Vibro-replacement stone column was designed in triangular pattern to mitigate liquefaction in this project. Take the 475-year return period earthquake as example, the parameters and critical values in design are listed in Table 5. The required minimum value of d/L is 0.45. Then stone columns with diameter of 0.5 m were installed at a column spacing of 1.1 m, the corresponding area replacement ratio is 0.1874 and the improvement depth is 16.8 m. Also, in zones with pile raft, the spacing L is set larger in consideration the additional densification effect induced by installation of pile raft.

The foundations of main buildings of the power plant sustain large load and have high requirement of deformation. Besides the use of stone column for liquefaction mitigation, pile raft was used in the same zone to control the foundation settlement (Fig. 9). It should be noted that the effect of overburden stress induced

Table 5 Critical values for stone column design (475-year return period)

Layer	Depth (m)	A	n	e_0	e_{cr}	d/L
1[a]	0.65	6.8	0.62	0.95	---	---
2	2.15	6.6	0.63	0.88	0.62	0.45
2	4.15	6.6	0.63	0.88	0.81	0.22
2	6.15	6.6	0.63	0.88	0.85	0.14
3	8.15	5.8	0.54	0.84	0.71	0.31
3	10.15	5.8	0.54	0.84	0.73	0.28
3	12.15	5.8	0.54	0.84	0.76	0.24
3	14.15	5.8	0.54	0.84	0.79	0.19

[a]The V_s- e correlation may not applicable for very shallow depth (e.g., d < 1 m)

by the pile raft foundation on liquefaction resistance of underlying soils could be expected beneficial. However, as the vertical overburden stress is designed to be carried by the piles beneath the raft, the possible influence of the raft is difficult to be evaluated and might be treated as an positive factor if there is any contact force between the raft and the soil surface. Figure 10 shows the feedback monitoring of stone column construction at the site. During the feedback monitor process, the diameter of stone column at a given elevation is visualized in PC real time according to the added volume of stone backfills, and then the densification quality could be secured or enhanced if necessary.

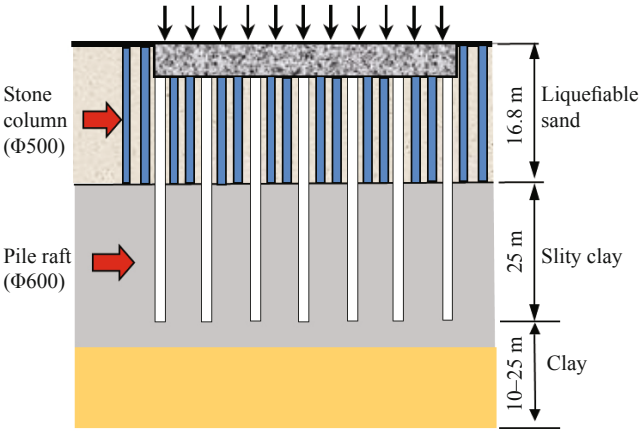

Fig. 9 Design of foundation for stone column and pile raft

4.4 Post-improvement liquefaction evaluation and seismic performance

To check the improvement quality, six SPT tests were performed in the shallow depth of surrounding soil (i.e., the upper 6.0 m) three months after the installation of stone columns. Figure 11 shows the post-improvement liquefaction evaluation of 475-year return period earthquake. Note that shear velocities used for CRR prediction are converted from SPT-N values according to Eq. (13) of Andrus *et al.* (2004), as there is no field V_s testing after improvement. Post-improvement CRR predicted by the present method is higher than CSR, which indicates that the site will not liquefy. Note that for depths of 3.15 m, 4.15 m and 5.15 m, the corrected SPT-N values (i.e., $N_{1,60}$) were larger than 30 and could be regarded as non-liquefiable. It could be found that the evaluations by the proposed V_s-based method agree well with NCEER SPT method.

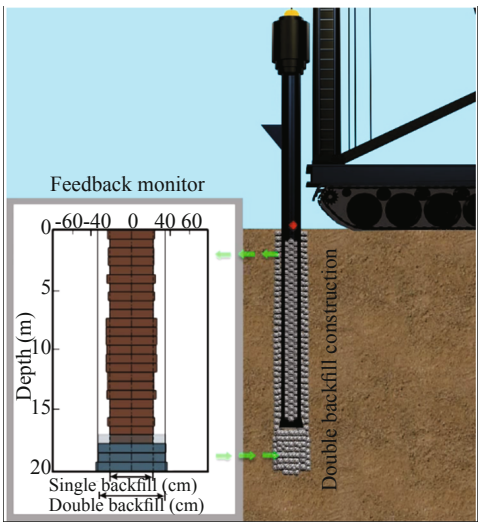

(a)

(b)

Fig.10 Stone column construction: (a) feedback monitoring; (b) construction at site

Very interestingly, a strong earthquake of magnitude M_w = 6.3 occurred about 25 km SSW of Yogyakarta, May 26, 2006, which epicenter is close to the project site. According to United States Geological Survey (USGS), the peak ground acceleration at this site was as high as 0.18 g. The stone column improved ground experienced no liquefaction (Fig. 12(a)), but severe liquefaction was observed in adjacent areas (e.g., Yogyakarta airport in Fig. 12(b)). The mitigation performance of stone column was validated by this strong earthquake.

4 Conclusions

The present study developed a procedure of V_s-based evaluation and design of stone column improved ground for liquefaction mitigation. Well-defined CRR-V_s and V_s-e correlations are proposed, together with the values of design parameters recommended for preliminary design when site specific values are not available. The procedures of pre- and post-improvement liquefaction evaluation and stone column design are given, and several design considerations according to mitigation mechanisms are provided for safety judgment. A case study of a thermal power plant in Indonesia is introduced to illustrate the site-specific design procedures, and the effectiveness of stone column improved ground was validated by strong earthquakes occurred after the completion of the project. The main findings of this study are as follows:

(1) Compared with existing methods recommended by design codes, the proposed method combining V_s and void ratio could secure physically meaningful and reliable criteria for stone column design for liquefaction mitigation. Besides the quality control process, the

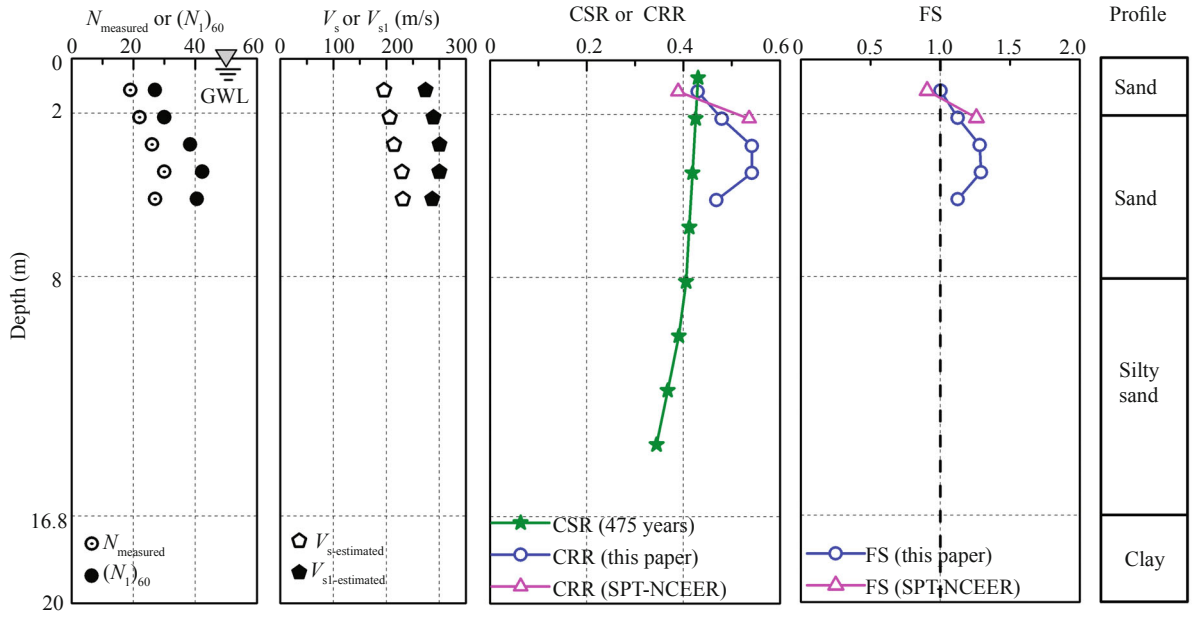

Fig. 11 Post-improvement liquefaction evaluation of 475-year earthquake return period

(a) (b)

Fig. 12 Seismic performance of the site: (a) with improvement; (b) without improvement

monitored V_s of pre- and post-improved ground also help the seismic response analyses of the ground when necessary.

(2) As this procedure relies on the densification of the surrounding soil instead of the whole improved ground, and excludes the drainage and reinforcement of stone columns, it could be regarded as conservative and the actual factor of safety after construction is expected higher. The high performance of liquefaction mitigation against strong earthquake in Indonesia described above supports this argument.

(3) The design and performance of stone column improved ground could be substantially enhanced by further researches and practices (e.g., physical and numerical modeling, and even field case studies). The mechanisms of densification, drainage and reinforcement of stone columns and their quantitative contributions to liquefaction resistance of treated soils need to be identified, and the time effect of construction disturbance should also be studied to interpret the post-improvement test properly.

Acknowledgment

This study is partly supported by the National Natural Science Foundation of China (No. 51578501, No. 51127005), the Foundation for the Author of National Excellent Doctoral Dissertation of P.R. China (No. 201160), the National Program for Special Support of Top-Notch Young Professionals (2013), the Zhejiang Provincial Natural Science Foundation of China (No. LR15E080001), the National Basic Research Program of China (973 Project) (No. 2014CB047005), the Fundamental Research Funds for the Central Universities (No. 2014FZA4016) and Zhejiang University K. P. Chao's High Technology Development Foundation (2014). All of the supports are greatly appreciated.

References

Aboshi H, Mizuno Y and Kuwabara M (1991), "Present State of Sand Compaction Pile in Japan," Deep Foundation Improvements: Design, Construction, and Testing, *ASTM Special Technical Publication*, **1089**: 32–46.

Adalier K and Elgamal A (2004), "Mitigation of Liquefaction and Associated Ground Deformations by Stone Columns," *Engineering Geology*, **72**(3–4): 275–291.

Alarcon-Guzman A, Chameau JL, Leonards GA, and Frost JD (1989), "Shear Modulus and Cyclic Undrained Behavior of Sands," *Soils and Foundations*, **29**(4):105–119.

Andrus RD, Piratheepan P, Ellis BS, Zhang JF and Juang CH (2004), "Comparing Liquefaction Evaluation Methods Using Penetration-V_s Relationships," *Soil Dynamics and Earthquake Engineering*, **24**(9–10): 713–721.

Andrus RD and Stokoe KH (2000), "Liquefaction Resistance of Soils from Shear-wave Velocity," *Journal of Geotechnical and Geoenvironmental Engineering*, ASCE, **126**(11): 1015–1025.

Baez JI (1995), "A Design Model for the Reduction of Soil Liquefaction by Vibro-stone Columns," *PhD Thesis*, University of Southern California, Los Angeles, CA, 207 pp.

Baez JI and Martin GR (1992), "Quantitative Evaluation of Stone Column Techniques for Earthquake Liquefaction Mitigation," *Proceedings of the Tenth World Conference on Earthquake Engineering*, Madrid, Spain, Vol. **3**: 1477–1483.

Boulanger R, Idriss I, Stewart D, Hashash Y and Schmidt B (1998), "Drainage Capacity of Stone Columns or Gravel Drains for Mitigating Liquefaction," *ASCE Geotechnical Special Publication*, No. **75**(1): 678–690.

Cai GJ, Liu SY and Puppala AJ (2012), "Liquefaction Assessments Using Seismic Piezocone Penetration (SCPTU) Test Investigations in Tangshan Region in China," *Soil Dynamics and Earthquake Engineering*, 41: 141–150.

Carriglio F (1989), "Caratteristiche Sforzi-deformazioni-resistenza delle Sabbie," *PhD Thesis*, Politecnico di Torino. (in Italian)

Chen YC and Lee CG (1994), "Evaluation of Liquefaction Resistance of Sand by Maximum Shear Modulus." *Journal of the Chinese Institute of Engineers*, **17**(5): 689–699.

Chen YM, Xu CX, Liu HL and Zhang WG (2015), "Physical Modeling of Lateral Spreading Induced by Inclined Sandy Foundation in the State of Zero Effective Stress," *Soil Dynamics and Earthquake Engineering*, **76**: 80–85.

Chung RM, Yokel FY and Drnevich VP (1984), "Evaluation of Dynamic Properties of Sands by Resonant Column Testing," *Geotechnical Testing Journal*, **7**(2): 60–69.

Conlee CT, Gallagher PM, Boulanger RW and Kamai R (2012), "Centrifuge Modeling for Liquefaction Mitigation Using Colloidal Silica Stabilizer," *Journal of Geotechnical and Geoenvironmental Engineering*, ASCE, **138**(11): 1334–1345.

Dabiri R, Askari F, Shafiee A and Jafari M (2011), "Shear Wave Velocity-based Liquefaction Resistance of Sand-silt Mixtures: Deterministic Versus Probabilistic Approach," *Iranian Journal of Science and Technology-Transaction of Civil Engineering*, **35**(2): 199–215.

Deb K and Shiyamalaa S (2015), "Effect of Clogging

on Rate of Consolidation of Stone Column–improved Ground by Considering Particle Migration," *International Journal of Geomechanics*, ASCE, DOI: 10.1061/(ASCE)GM.1943-5622.0000492, 04015017.

Dobry R, Ladd RS, Yokel FY, Chung RM and Powell D (1982), "Prediction of Pore Water Pressure Buildup and Liquefaction of Sands during Earthquakes by the Cyclic Strain Method," National Bureau of Standards Building Sci. Ser, U.S., 138 Washington, DC.

Durgunoglu, HT (2006), "Utilization of High Modulus Columns in Foundation Engineering under Seismic Loadings," *U.S. 8th National Conf. on Earthquake Engineering*, *Earthquake Engineering Research Institute*, San Francisco.

Elgamal A, Lu J and Forcellini D (2009), "Mitigation of Liquefaction-induced lateral deformation in a sloping stratum: three-dimensional numerical simulation," *Journal of Geotechnical and Geoenvironmental Engineering*, ASCE, **135**(11): 1672–1682.

European Committee for Standardization EN 1998-5:2004 (2004), "Eurocode 8: Design of Structures for Earthquake Resistance—part 1: General rules, Seismic Actions and Rules for Buildings," *European Committee of standardization*, Brussels.

Harada K, Orense RP, Ishihara K and Mukai J (2010), "Lateral Stress Effects on Liquefaction Resistance Correlations," *Bulletin of the New Zealand Society for Earthquake Engineering*, **43**(1): 13–23.

Hardin BO and Richart FEJ (1963), "Elastic Wave Velocities in Granular Soils," *Journal of Soil Mechanics and Foundations Div*., ASCE, **89**(1): 33–65.

Howell R, Rathje EM, Kamai R and Boulanger R (2012), "Centrifuge Modeling of Prefabricated Vertical Drains for Liquefaction Remediation," *Journal of Geotechnical and Geoenvironmental Engineering*, ASCE, **138**(3): 262–271.

Huang MS, Chen YM and Wu SM (1992), "Test Research on Silty Sand Ground Densification by Vibro-stone Column," *Chinese Journal of Geotechnical Engineering*, **14**(6): 69–73. (in Chinese)

Huang YT, Huang AB, Kuo YC and Tsai MD (2004), "A Laboratory Study on the Undrained Strength of a Silty Sand from Central Western Taiwan," *Soil Dynamics and Earthquake Engineering*, **24**(9): 733–743.

Iai S, Koizumi K, Noda S and Tsuchida H (1988), "Large Scale Model Tests and Analysis of Gravel Drains," *Report of the Port and Harbour Research Institute*, **27**(3): 0–2.

Iwasaki T and Tatsuoka F (1977), "Effects of Grain Size and Grading on Dynamic Shear Moduli of Sands," *Soils and Foundations*, **17**(3): 19–35.

Iyengar M (1981), "Improvement of Characteristics of a Liquefiable Soil Deposits by Pile Driving Operations," *First International Conference on Recent Advances in Geotechnical earthquake Engineering and Soil Dynamics*, Missouri S&T.

Japanese Geotechnical Society (1998), "Remedial Measures against Soil Liquefaction," A.A. Balkema, Rotterdam, Netherlands.

Jin JJ, Zhang HR, Huang CX and Yuan ZH (2008), "Experimental Study on Liquefiable Foundation Improved by Stone Columns Under Cyclic Loading," *Journal of Beijing Jiaotong University*, **32**(4): 111–115.

Jovicic V and Coop MR (1997), "Stiffness of Coarse Grained Soils at Small Strains," *Geotechnique*, **47**(3): 545–561.

Juang CH, Chen CJ and Jiang T (2001), "Probabilistic Framework for Liquefaction Potential by Shear Wave Velocity," *Journal of Geotechnical and Geoenvironmental Engineering*, ASCE, **127**(8): 670–678.

Kayen R, Moss R, Thompson E, Seed R, Cetin K, Kiureghian AD, Tanaka Y, and Tokimatsu K (2013), "Shear-wave Velocity–based Probabilistic and Deterministic Assessment of Seismic Soil Liquefaction Potential," *Journal of Geotechnical and Geoenvironmental Engineering*, ASCE, **139**(3):407–419.

Kokusho T (1980), "Cyclic Triaxial Test of Dynamic Soil Properties for Wide Strain Range," *Soils and Foundations*, **20**(2): 45–60.

Laird JP and Stokoe KH (1993), "Dynamic Properties of Remolded and Undisturbed Soil Samples Tested at High Confining Pressures," *Report GR93-6, Electric Power Research Institute*, Palo Alto, Calif., USA.

Liu SY, Fang L and Hu XF (2000), "Experimental Study on Liquefiable Foundation Reinforeced with Dry-vibro Gravel Piles," *Journal of Engineering Geology*, **2000**(4): 488–492. (in Chinese)

Lo Presti DCF (1987), ''Mechanical Behavior of Ticino Sand from Resonant Column Tests,'' *PhD Thesis*, Politecnico di Torino, Turin, Italy.

Lo Presti DCF, Jamiolkowski M, Pallara O, Cavallaro A and Pedroni M (1997), "Shear Modulus and Damping of Soils," *Geotechnique*, **47**(3): 603–617.

Lukas RG (1997), "Delayed Soil Improvement after Dynamic Compaction," *ASCE Geotechnical Special Publication*, No. 69, pp. 409–420.

Ministry of Housing and Urban-rural Development of the People's Republic of China (2009), *Code for Investigation of Geotechnical Engineering* (*GB50021-2001*), China Architecture and Building Press. (in Chinese)

Ministry of Housing and Urban-rural Development of the People's Republic of China (2009), *Code for Engineering Geological Investigation of Water*

Resources and Hydropower (GB50487-2008), China Planning Press. (in Chinese)

Ministry of Housing and Urban-rural Development of the People's Republic of China (2010), *Code for Seismic Design of Buildings* (*GB50011-2010*), China Architecture and Building Press. (in Chinese)

Mitchell JK, Baxter CDP and Munson TC (1995), "Performance of Improved Ground during Earthquakes," *Soil Improvement for Earthquake Hazard Mitigation* (GSP 49), ASCE, San Diego, CA: 1–36.

Mitchell JK and Solymar ZV (1984), "Time-dependent Strength Gain in Freshly Deposited or Densified Sand," *Journal of Geotechnical Engineering*, ASCE, **110**(11), 1559–1576.

NEHRP (2003), *FEMA 450—NEHRP Recommended Provisions for Seismic Regulation for New Buildings and other Structures*, Federal Emergency Management Agency, Washington, DC.

Nuclear Regulatory Commission NUREG/CR-5741 (2000), *Technical Bases for Regulatory Guide for Soil Liquefaction*, J.P. Koester, M.K. Sharp, M.E. Hynes, Editors, USNRC.

Özener P (2012), "Estimation of Residual Shear Strength Ratios of Liquefied Soil Deposits from Shear Wave Velocity," *Earthquake Engineering and Engineering Vibration*, **11**(4): 461–484.

Pan H, Chen GX, Liu HL and Wang BH (2011), "Behavior of Large Post-liquefaction Deformation in Saturated Nanjing Fine Sand," *Earthquake Engineering and Engineering Vibration*, **10**(2): 187–193.

Paydar NA and Ahmadi M (2014), "Influence of Fines Content and Type on the Small-strain Shear Modulus of Sand," *Scientia Iranica, Transaction A, Civil Engineering*, **21**(4): 1281–1296.

Rayamajhi D, Nguyen TV, Ashford SA, Boulanger RW, Lu J, Elgamal A and Shao L (2012), "Effect of Discrete Columns on Shear Stress Distribution in Liquefiable Soil," *GeoCongress*, 1908–1917.

Rayamajhi D, Tamura S, Khosravi M, Boulanger RW, Wilson DW, Ashford SA and Olgun CG (2015), "Dynamic Centrifuge Tests to Evaluate Reinforcing Mechanisms of Soil-cement Columns in Liquefiable Sand," *Journal of Geotechnical and Geoenvironmental Engineering*, 10.1061/(ASCE)GT.1943-5606.0001298.

Robertson P, Woeller D and Finn W (1992), "Seismic Cone Penetration Test for Evaluating Liquefaction Potential under Cyclic Loading," *Canadian Geotechnical Journal*, **29**(4): 686–695.

Salgado R, Bandini P and Karim A (2000), "Shear Strength and Stiffness of Silty Sand," *Journal of Geotechnical and Geoenvironmental Engineering*, ASCE, **126**(5): 451–462.

Samui P (2007), "Seismic Liquefaction Potential Assessment by Using Relevance Vector Machine," *Earthquake Engineering and Engineering Vibration*, **6**(4): 331–336.

Seed HB and Booker JR (1977), "Stabilization of Potentially Liquefiable Sand Deposits Using Gravel Drains," *Journal of Geotechnical Engineering Division*, **103**(7): 757–768.

Seed HB and Idriss IM (1971), "Simplified Procedure for Evaluating Soil Liquefaction Potential," *Journal of Soil Mechanics and Foundations Division*, **97**(9): 1249–273.

Shenthan T, Nashed R, Thevanayagam S and Martin GR (2004), "Liquefaction Mitigation in Silty Soils Using Composite Stone Columns and Dynamic Compaction," *Earthquake Engineering and Engineering Vibration*, **3**(1): 39–50.

Shi ZJ, Yu SS and Feng WL (1993), "Evaluation of Liquefaction Potential by Shear Wave Velocity," *Chinese Journal of Geotechnical Engineering*, **15**(1): 74–80. (in Chinese)

Skoglund GR, Cunny RW and Marcuson WF (1976), "Evaluation of Rsonant Column Test Devices," *Journal of Geotechnical and Engineering Division*, ASCE, **102**(11): 1147–1158.

Stuedlein AW, Abdollahi A, Mason HB and French R (2015), "Shear Wave Velocity Measurements of Stone Column Improved Ground and Effect on Site Response," Proc., IFCEE 2015, pp.2306–2317.

Tang L, Lin XZ, Xu PJ, Gao X and Wang DS (2014), "Response of a Pile Group behind Quay Wall to Liquefaction-induced Lateral Spreading: a Shake-table Investigation," *Earthquake Engineering and Engineering Vibration*, **13**(4): 741–749.

Tang L, Zhang XY and Ling XZ (2015), "Numerical Simulation of Centrifuge Experiments on Liquefaction Mitigation of Silty Soils using Stone Columns," *KSCE Journal of Civil Engineering, Geotechnical Engineering*, DOI 10.1007/s12205-015-0363-7.

Tokimatsu K and Uchida A (1990), "Correlation between Liquefaction Resistance and Shear Wave Velocity," *Soils and Foundations*, **30**(2): 33–42.

Wang WS (2001), "Utilization of Shear Wave Velocity in Assessment of Liquefaction Potential of Saturated Sand under Level Ground During Earthquakes," *Chinese Journal of Geotechnical Engineering*, **23**(6): 659–662. (in Chinese)

Wang BH, Chen GX and Jin DD (2010), "Pore Water Pressure Increment Model for Saturated Nanjing Fine Sand Subject to Cyclic Loading," *Earthquake Engineering and Engineering Vibration*, **9**(4): 569–576.

Wang LM, He KM, Shi YC and Wang J (2002), "Study on Liquefaction of Saturated Loess by In-situ Explosion Test," *Earthquake Engineering and Engineering*

Vibration, 2002, **1**(1): 50–56.

Wichtmann T and Triantafyllidis T (2009), "Influence of the Grain-size Distribution Curve of Quartz Sand on the small Strain Shear Modulus G_{max}," *Journal of Geotechnical and Geoenvironmental Engineering*, ASCE, **135**(10): 1404–1418.

Yamashita S, Ito Y, Hori T, Suzuki T and Murata Y (2003), "Geotechnical Properties of Liquefied Volcanic Soil Ground by 2003 Tokachi-oki Earthquake." *Proc., Proceedings of the International Conference on Soil Mechanics and Geotechnical Engineering*, AA Balkema Publishers, 2737.

Yasuda N and Matsumoto N (1993), "Dynamic Deformation Characteristics of Sands and Rockfill Materials," *Canadian Geotechnical Journal*, **30**(5): 747–757.

Yoon YW and Van Impe WF (1995), "Dynamic Behavior of Crushable Sand," *First Int. Conf. on Earthquake Geotechnical Engineering, A. A. Balkema, The Netherlands*, 227–232.

Youd TL, Idriss IM, Andrus RD, *et al*. (2001), "Liquefaction Resistance of Soils: Summary Report from the 1996 NCEER and 1998 NCEER/NSF Workshops on Evaluation of Liquefaction Resistance of Soils," *Journal of Geotechnical and Geoenvironmental Engineering*, ASCE, **127**(10): 817–833.

Yuan XM and Cao ZZ (2001), "A Fundamental Procedure and Calculation Formula for Evaluating Gravel Liquefaction," *Earthquake Engineering and Engineering Vibration*, **10**(3): 339–347.

Zhang YM and Zhang HR (2008), "Influence of Stone Columns Design Parameters on Anti-liquefaction Nature of Composite Foundation," *Rock and Soil Mechanics*, **29**(5): 1320–1325.

Zhou YG and Chen YM (2007), "Laboratory Investigation on Assessing Liquefaction Resistance of Sandy Soils by Shear Wave Velocity," *Journal of Geotechnical and Geoenvironmental Engineering*, ASCE, **133**(8): 959–972.

Zhou YG, Chen YM and Ling DS (2009), "Shear Wave Velocity-based Liquefaction Evaluation in the Great Wenchuan Earthquake: a Preliminary Case Study". *Earthquake Engineering and Engineering Vibration*, **8**(2): 231–239.

Zhou YG, Chen YM and Shamoto Y (2010), "Verification of the Soil-type Specific Correlation between Liquefaction Resistance and Shear-wave Velocity of Sand by Dynamic Centrifuge Test", *Journal of Geotechnical and Geoenvironmental Engineering*, ASCE, **136**(1): 165–177.

Zhou J, Wang ZH, Chen XL and Zhang J (2014), "Uplift Mechanism for a Shallow-buried Structure in Liquefiable Sand Subjected to Seismic Load: Centrifuge Model Test and DEM Modeling," *Earthquake Engineering and Engineering Vibration*, **13**(2): 203–214.

Appendix:

Database for obtaining parameters of *A* and *n*

Table A1 Parameter of Hardin equation for different sandy soils

Sand type	FC(%)	*A*	*n*	Reference
Ottawa sand (S1)	0	47–500	0.50	Alarcon-Guzman *et al*. (1989)
Ottawa sand (S2)	0	560–600	0.50	Hardin and Richart (1963)
Monterey NO.0 sand (S3)	0	520	0.48	Chung *et al*. (1984)
Monterey NO.0 sand (S4)	0	420	0.57	Saxena and Reddy
Hokksund sand (S5)	0	560–570	0.50[a]	Carriglio (1989)
Iruma sand (S6)	0	690	0.50	Iwasaki and Tatsuoka (1977)
Quiou sand (S7)	0	660–700	0.62	Lo Presti *et al*. (1997)
Rockfill sand (S8)	0	470–550	0.50[a]	Yasuda and Matsumoto (1993)
Ticino sand (S9)	0	580	0.48	Carriglio (1989)
Ticino sand (S10)	0	370–500	0.46	Cho *et al*.
Nevada sand (S11)	0	490	0.48	Cho *et al*.
Toyoura sand (S12)	0	700–720	0.50	Kokusho (1980)
Toyoura sand (S13)	0	700–720	0.50[a]	Lo Presti *et al*. (1997)
Antewerp (S14)	0	420–460	0.50[a]	Yoon and Van Impe (1995)
Ham River sand (S15)	0	550	0.50[a]	Jovicic and Coop (1997)
Mortal sand (S16)	0	625	0.50[a]	Laird and Stokoe (1993)
Mol sand (S17)	0	655–670	0.50[a]	Yoon and Van Impe (1995)
Reid-Bedford sand (S18)	0	580	0.50[a]	Skoglund *et al*. (1976)

Sand type	FC(%)	*A*	*n*	Reference
Firoozkooh sand (S19)	0	420–490	0.48	Paydar and Ahmadi (2014)
Margaret river sand (S20)	0	580–780	0.44	Cho *et al*.
ASTM 20/30 sand (S21)	0	360	0.50	Cho *et al*.
Sandboil sand (S22)	0	400–550	0.48	Patel *et al*.
Daytona sand (S23)	0	440–600	0.48	Patel *et al*.
Fraser sand (S24)	0	310–420	0.56	Patel *et al*.
Michigan sand (S25)	0	420–560	0.44	Patel *et al*.
Syncrude sand (S26)	0	400–530	0.50	Patel *et al*.
Dorsten sand (S27)	0	680–800	0.43	Wichtmann and Triantafyllidis (2009)
Dorsten sand (S28)	0	700–820	0.42	Wichtmann and Triantafyllidis (2009)
Dorsten sand (S29)	0	800–880	0.41	Wichtmann and Triantafyllidis (2009)
Dorsten sand (S30)	0	740–800	0.43	Wichtmann and Triantafyllidis (2009)
Dorsten sand (S31)	0	700–780	0.43	Wichtmann and Triantafyllidis (2009)
Dorsten sand (S32)	0	660–710	0.45	Wichtmann and Triantafyllidis (2009)
Dorsten sand (S33)	0	600–640	0.45	Wichtmann and Triantafyllidis (2009)
Dorsten sand (S34)	0	600–700	0.46	Wichtmann and Triantafyllidis (2009)
Dorsten sand (S35)	0	500–670	0.48	Wichtmann and Triantafyllidis (2009)
Dorsten sand (S36)	0	450–620	0.50	Wichtmann and Triantafyllidis (2009)
Dorsten sand (S37)	0	360–560	0.51	Wichtmann and Triantafyllidis (2009)
Dorsten sand (S38)	0	330–500	0.54	Wichtmann and Triantafyllidis (2009)
Dorsten sand (S39)	0	250–470	0.53	Wichtmann and Triantafyllidis (2009)
Dorsten sand (S40)	0	600–680	0.47	Wichtmann and Triantafyllidis (2009)
Dorsten sand (S41)	0	540–630	0.48	Wichtmann and Triantafyllidis (2009)
Dorsten sand (S42)	0	410–610	0.49	Wichtmann and Triantafyllidis (2009)
Dorsten sand (S43)	0	430–510	0.51	Wichtmann and Triantafyllidis (2009)
Dorsten sand (S44)	0	370–480	0.54	Wichtmann and Triantafyllidis (2009)
Dorsten sand (S45)	0	260–450	0.55	Wichtmann and Triantafyllidis (2009)
Dorsten sand (S46)	0	300–410	0.58	Wichtmann and Triantafyllidis (2009)
Dorsten sand (S47)	0	630–730	0.43	Wichtmann and Triantafyllidis (2009)
Dorsten sand (S48)	0	560–680	0.44	Wichtmann and Triantafyllidis (2009)
Dorsten sand (S49)	2	300–450	0.54	Wichtmann and Triantafyllidis (2009)
Dorsten sand (S50)	8	480–660	0.46	Wichtmann and Triantafyllidis (2009)
Dorsten sand (S51)	16	620–680	0.44	Wichtmann and Triantafyllidis (2009)
Lanyang sand (S52)	10	400	0.65	Chen and Lee (1994)
Mailiao sand (S53)	5	450–460	0.50	Huang *et al*.
Mailiao sand (S54)	10	350–370	0.50	Huang *et al*.
Mailiao sand (S55)	15	260–290	0.50	Huang *et al*.
Firoozkooh sand (S56)	15	250–330	0.52	Paydar and Ahmadi (2014)
Firoozkooh sand (S57)	25	200–300	0.50	Paydar and Ahmadi (2014)
Firoozkooh sand (S58)	30	340	0.50[a]	Dabiri *et al*. (2011)
Firoozkooh sand (S59)	35	200	0.48	Paydar and Ahmadi (2014)
Firoozkooh sand (S60)	50	170	0.65	Paydar and Ahmadi (2014)
Firoozkooh sand (S61)	75	230	0.60	Paydar and Ahmadi (2014)

[a]Assumed *n* for calculation due to lack of available information